frontiers | Frontiers in Earth Science

TYPE Original Research
PUBLISHED 03 December 2024
DOI 10.3389/feart.2024.1503646

Analysis of genetic sandbodies and coal seams with coal-bearing of Middle-Lower Jurassic in the Junggar Basin

Yao Zongquan[1]*, Wang Wei[1], Wang Yong[2], Xie Zongrui[3], Yang Xingtao[3], Yang Fan[4] and Zhou Qihao[5]

[1]Xinjiang University, Urumqi, China, [2]Research Institute of Petroleum Exploration and Development, SINOPEC Shengli Oilfield Company, Dongying, Shandong, China, [3]Xinjiang Oilfield Company, Karamay, Xinjiang Uyghur Autonomous Region, China, [4]Research Institute of Peleoleum Exploration and Development, PetroChina, Beijing, China, [5]The University of Utah, Salt LakeCity, UT, United States

OPEN ACCESS

EDITED BY
Hongjian Zhu,
Yanshan University, China

REVIEWED BY
Peng Qiao,
China Geological Survey, China
Kyiazbek Asilbekov,
National Academy of Sciences of Kyrgyz Republic, Kyrgyzstan

*CORRESPONDENCE
Yao Zongquan,
yzq@xju.edu.cn

RECEIVED 29 September 2024
ACCEPTED 11 November 2024
PUBLISHED 03 December 2024

CITATION
Zongquan Y, Wei W, Yong W, Zongrui X, Xingtao Y, Fan Y and Qihao Z (2024) Analysis of genetic sandbodies and coal seams with coal-bearing of Middle-Lower Jurassic in the Junggar Basin.
Front. Earth Sci. 12:1503646.
doi: 10.3389/feart.2024.1503646

Introduction: The sediment genetic mechanisms have always been an important branch of the "source-sink" system, and it is also a research hotspot.

Methods: Conglomerate, sandstone, and coal are developed of Middle-Lower Jurassic in the Junggar Basin, and the genetic mechanism is not clear, which restricts further exploration of oilfield. Based on the core carefully, test data, and outcrop sections, Badaowan and Xishanyao formations are analyzed.

Results: Five types of conglomerate lithofacies and sandstone lithofacies, two kinds of mudstone lithofacies, and one type of coal are identified. Based on the structural-genetic mechanism, the debris flow and traction current with conglomerate are developed, and a method of the semi-quantitative identifying index is proposed based on the sedimentary sequence of lithological characteristics, MPS/BTh, and grain size characteristics as the identification criteria. Depending on fluvio-delta, the genetic bodies of the distribution channel, subaqueous distribution channel, mouth bar, braided channel, and overbank sandstone are divided.

Discussion: By integrating structural, paleoclimatic, and sedimentary environment, it was observed that coal in the Badaowan Formation has the characteristics of continuous and stable distribution of thick layers, whereas multiple sets of discontinuous and instable distribution are observed in the in Xishanyao Formation. Finally, the filling model is established, and the superposition and distribution of sandbodies are clarified.

KEYWORDS

lithofacies, sediment genetic, coal-bearing, Middle-Lower Jurassic, Hongshanzui area, Junggar

1 Introduction

The "source-sink" system is a research hotspot (Allen et al., 2016), and the sedimentary genetic mechanism, as an important branch, has made great progress in recent years (Zhu et al., 2023). In the mid-1990s, with the emergence of clastic flow deposits in outcrops and cores that cannot be explained by the turbidity current theory, scholars and experts began to re-understand the deepwater deposition process. Debris flow deposition was first studied systematically by Johnson (1965). Afterward, A (1972) established the relationship between sliding debris flow and turbidity currents. Middleton and Hampton (1976) divided gravity flow into liquefied flow, granular flow, debris flow, and turbidity flow. As Postma (1990) separated the debris flow from the high-density turbidity current by physical simulation, further advancements have been made in theory and sedimentary examples (Weaver et al., 2007; Georgiopoulou, 2013). Subsequently, Shanmugam (2000) proposed sandy debris flow and defined the fluid properties, state and transport mechanism. Domestic scholars and experts have also carried out related research on the sedimentary characteristics of debris flow (Zhang et al., 2014; Zhu et al., 2021), the relationship between turbidity currents and sandy debris flow (Pei et al., 2015), the genetic mechanisms (Cao et al., 2017), the genetic model (Xian et al., 2013; Li et al., 2014; Yuan, 2016), and the type of gravity flow (Yang et al., 2015). Xian et al. (2014) divided the gravity flow into five stages based on statistics published by Elsevier Science and GSE journals. Before 1950, random observation stage; 1950s–60s, the establishment stage of the conceptual system; in the 1970s, the establishment stage of sedimentary models; 1980–1995, industrial application and questioning stage; and 1996–present, debris flow research stage (Xian et al., 2014).

The Hongshanzui oilfield belongs to the complex large-scale fault block area under the background of lake basin sedimentation. Over the years, many scholars and experts have focused on the structural characteristics, sedimentary environment, reservoir physical properties, and reservoir description, and they have clarified that the Jurassic period is a depression basin with a topographic slope break zone (Meng et al., 2009), and determined that its lithology is dominated by gravelly sandstone (Hu and Zhu, 2002). They have identified four III sequences of the Jurassic system, mainly developing alluvial fans and braided river deltas (Hu and Li, 2003). However, there are few articles on the genetic mechanism of structural-genetic conglomerates (Yao et al., 2019). For the genesis of sandstone bodies, it is mainly concentrated on the sand lithofacies (Liu et al., 2018), or mixed with conglomerate bodies; there is a lack of special research on the genesis of sandbodies, especially in the Hongshanzui area. The main viewpoint on the genesis of coal seams is to conduct research on the laws of coal accumulation within a sequence framework, analyzing the control of the balance between the rate of accommodation space change and the rate of peat accumulation on coal seams (Diessel et al., 2000; Wang et al., 2019; Zhang et al., 2019). Shao et al. (2017) further clarified that coal accumulation is controlled by paleostructure and sedimentary environment. However, the genesis of Jurassic thick and thin coal seams and continuous and discontinuous coal seams in the northwestern margin of the Junggar Basin has not been reported.

In view of the shortcomings in the above research, in this paper, we analyze the lithofacies, dissect the genetic glutenite bodies under different sedimentary systems, clarify the mechanism and distribution patterns of sandbodies, and provide theoretical guidance for the fine exploration of the Middle and Lower Jurassic in the Hongshanzui oilfield.

2 Study area

The northwestern edge of the Junggar Basin is located in the basin mountain transition zone between Hala'alate Mountain and the southern part of the Zaire mountains. It starts from the Delun Mountain in the north and reaches Ebinur Lake in the south. It is generally NE-trending and is now an uplift zone. It is adjacent to the Mahu depression, Changji depression, and Sikeshu depression. Tectonically, the Kebai fault zone and Hongche fault zone are successively developed from north to south (Sui, 2015). The Hongshanzui oilfield, located in the northwestern margin of the Junggar Basin, is a complex large fault block area cut by many faults and belongs to the uplift tectonic unit in the west of the Junggar Basin (Meng et al., 2009). Its structural location is in the north of the Hongche fault zone; during the Hercynian and Indosinian movements, the fault block area was affected by the extrusion from northwest to southeast, resulting in multi-stage reverse faults. The faults are all developed from the basement and contemporaneous, resulting in the sedimentary discontinuity between the Jurassic Badaowan Formation and the Triassic System (Figures 1A, B).

The target object in the study area is the Jurassic, including the J_1b, J_1s, J_2x, J_2t, and J_3q. The underlying T_3b is in conformable contact and the overlying K_1tg is in unconformable contact (Figure 1C). The J_1s is mainly composed of a large set of mudstones, without the development of sandstone and coal seams, so it is not the object of this study. J_1b can be divided into five sections: the J_1b_5, J_1b_4, J_1b_3, J_1b_1, and J_1b_2 region missing. J_2x can be divided into the J_2x_1, J_2x_2, J_2x_3, and J_2x_4 (Figure 1D). The formation is gradually denuded and thinned to the southwest and even missing, such as loss of erosion in the J_2x_4 of the Hong91 well area in the south, and only the remaining J_2x_1 in the Hong43 well area. Boulder clay can be seen at the bottom of the J_2x, with developed coal seams and abundant plant fossils (Li et al., 2014; Yao et al., 2019). Field outcrops are well exposed in the front of the Zaire mountains.

3 Data and method

The core well data, logging data, core photos, and seismic data used in this research belong to the Exploration and Development Research Institute of Xinjiang Oilfield Company, and the outcrop is selected in the Zaire mountains with good exposure.

Refer to Porêbski (1981) for the classification of MPS/BTh conglomerate. The cumulative curve of particle size probability is drawn by the sieving analysis method. The identification and division of lithofacies are mainly based on the realistic core description, the quantitative judgment and classification of the main types of lithofacies by the three-end element method, and the auxiliary naming method by the significant sedimentary structural, paleontological, and fabric characteristics.

4 Results

4.1 Lithofacies

The lithofacies is a rock combination with special sedimentary structures, reflecting the process of natural sorting and unloading

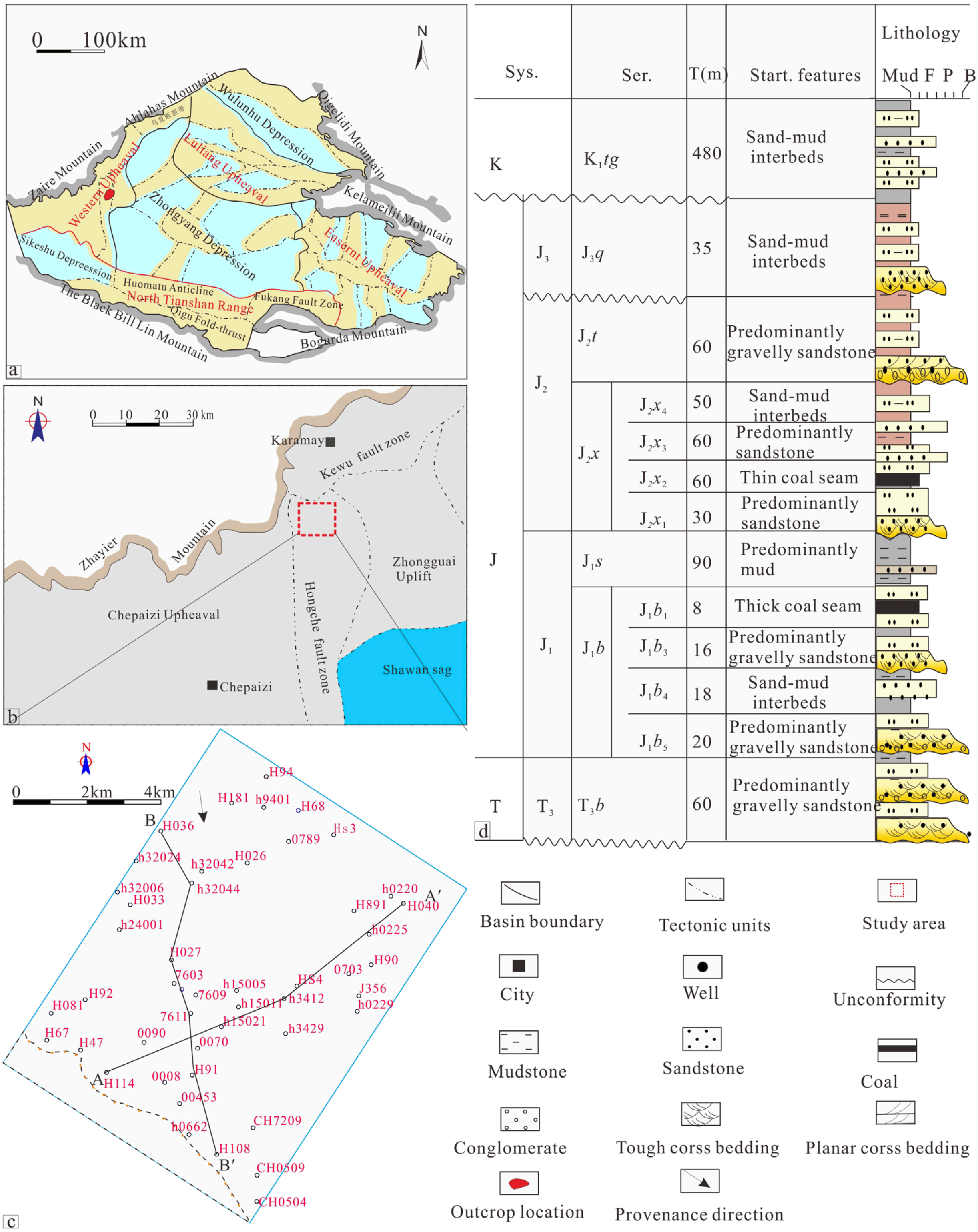

FIGURE 1
Location, tectonic, and stratigraphic log of Hongshanzui area in the Junggar Basin. **(A)** Junggar Basin, the selected outcrop section located in northwestern margin of the Junggar Basin (red area). **(B)** Study area (red dashed box). **(C)** Distribution of key well. **(D)** Integrated stratigraphic column.

of sediments, which represents the energy unit of sedimentary hydrodynamic condition (Miall, Andrew D, 1996). This article is based on the lithofacies classification program (Hemmesch et al., 2014): the Middle-Lower Jurassic in the Hongshanzui area is finely divided into 13 lithofacies, including five kinds of conglomerate lithofacies, five kinds of sandstone lithofacies,

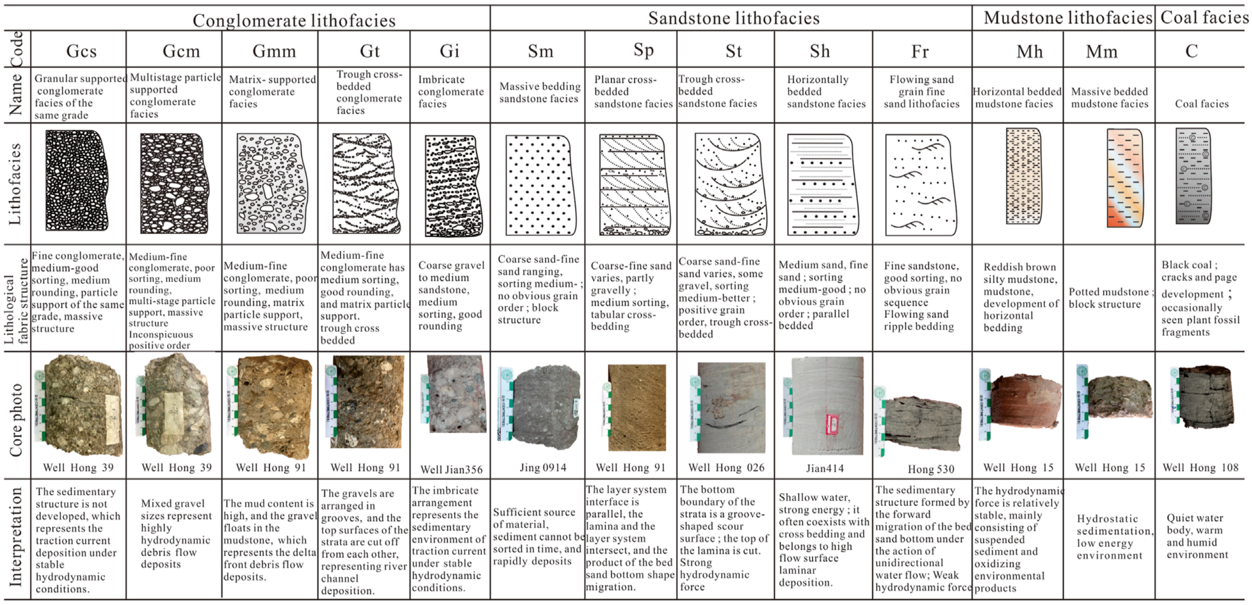

FIGURE 2
Lithofacies types with coal-bearing strata of Middle-Lower Jurassic in Hongshanzui area in the Junggar Basin.

two kinds of mudstone lithofacies, and one kind of coal lithofacies.

4.1.1 Conglomerate lithofacies

Based on the support forms, grain size, and arrangement of gravel particles within the study area, five kinds of conglomerate lithofacies are identified: Gcs, Gcm, Gmm, Gt, and Gi (Figure 2).

4.1.1.1 Same-grade particle-supported conglomerate facies (Gcs)

The lithofacies is mainly medium-fine conglomerate, with good compositional and structural maturity of conglomerates. The particles support and contact each other, and sedimentary structures are rare. It developed in distributary channel and underwater distributary channel, representing the traction flow deposits under stable hydrodynamic conditions (Tan et al., 2017).

4.1.1.2 Multi-stage particle-supported conglomerate facies (Gcm)

The conglomerate of lithofacies are mixed in size, and poorly sorted and rounded. The cobble is filled with pebble, granule, and sandstone. The gravel particles are supported by multi-stage particles, which represent the sedimentary environment of the gravity flow of the delta plain distributary channel with strong hydrodynamic, short transport distance, and rapid accumulation (Zhang et al., 2020).

4.1.1.3 Matrix-supported conglomerate facies (Gmm)

According to the lithological differences, the matrix-supported conglomerate facies in the study area can be divided into matrix-supported and sandy-supported conglomerate facies. Among them, the matrix-supported conglomerate facies, which is characterized by high mud content, is the conglomerate predominantly floating within the muddy matrix, indicative of the distributary channel environment formed by deltaic delta gravity flows. The medium-fine sandstone is filled between the gravel particles in the sandy-supported conglomerate facies, which often represents the subaqueous distributary channel deposits at the delta front. Occasionally, conglomerates are vertically distributed within the matrix, indicating that gravitational sorting occurred in the sedimentary environment at that time.

4.1.1.4 Trough cross-bedded conglomerate facies (Gt)

The identifying characteristics of this lithofacies are that the layers' interface is filled with pebble and granule, and the laminae are filled with secondary-order or sandstone. There are mutual truncations between layers and laminas. The particles are filled with muddy and sandstone, and lagging can be seen at the bottom of the trough, with a clear scouring surface. The orientation of the trough reflects the direction of water flow, typically formed by erosion and filling of distributary channels at the delta front (Khadkikar et al., 1999).

4.1.1.5 Imbricated conglomerate facies (Gi)

The conglomerates are arranged in an imbricate direction, with particles supporting, and the particles are mostly filled with matrix. It is generally sorted, well rounded, and often associated with massive bedding, representing the sedimentary environment of traction flow under stable hydrodynamic conditions, and often appears at the bottom of the underwater distributary channel at the delta front.

4.1.2 Sandstone lithofacies

The study area identified a total of five sandstone lithofacies, namely, Sm, Sp, St, Sh, and Fr (Figure 2).

4.1.2.1 Massive-bedded sandstone facies (Sm)

It is mainly composed of medium-fine sandstone, with relatively homogeneous lithology, showing no obvious sedimentary structural. It is usually formed when the sediment is deposited without significant sorting under the condition of abundant sediment supply, and is commonly more common in braided channel environment.

4.1.2.2 Planar cross-bedded sandstone facies (Sp)

The stratigraphic boundaries of this type of lithofacies are filled with coarser sandstone, whereas the laminae are filled with finer sandstone. The strata and lamina are truncations of each other, which is the product of the migration of two-dimensional bed sand. The wave ridge shape is linear, and the superposition of multiple sets of Sp overlap can be judged as mouth bar (Soltan and Mountney, 2016).

4.1.2.3 Trough cross-bedded sandstone facies (St)

The sedimentary base boundary typically exhibits "spoon-shaped" morphology, and some granules are usually distributed along the layer at the bottom of the trough, creating an uneven surface. The bedforms can appear tongue-shaped or crescent-shaped (Allen, 1983). It is the product of three-dimensional bed sand bottom migration, which is commonly found at the bottom of delta channels, reflecting the process of the channel scouring and filling.

4.1.2.4 Parallel-bedded sandstone facies (Sh)

This lithofacies is primarily composed of medium-fine sandstone. Its defining characteristic is the overlapping of grains within laminae. It forms in shallow water, high-energy environments under traction currents, and often coexists with cross-bedded, indicating the channel filling deposition (Allen, 1982).

4.1.2.5 Rippled laminated fine sandstone facies (Fr)

Primarily composed of fine-grained sandstone with good sorting, it consists of superimposed ripple textures formed by migrating water flow and simultaneous upward growth, which are mostly occurring in the later stage of channel evolution.

4.1.3 Mudstone lithofacies

There are primarily two types of mudstone facies in the study area, the Mh and the Mm (Figure 2).

4.1.3.1 Horizontal bedded mudstone facies (Mh)

This type of lithofacies is formed by suspension precipitation in a low-energy sedimentary environment with relatively weak and stable hydrodynamic conditions (Gao et al., 2024). This lithofacies appears red in color, representing a swampy environment dominated by terrestrial oxidation conditions.

4.1.3.2 Massive bedded mudstone facies (Mm)

This type of mudstone is lacking visible bedding structures, which is mainly formed by suspension sedimentation. Due to the changes in the content of Fe^{3+} and OH^{-} of pore water and diffusion within the sediment, variegated block-layered mudstone facies can be seen. Additionally, gray mudstone facies are present, indicating a sedimentary environment enriched organic matter. These typically represent sedimentation often characterized by anoxic conditions, top of single-cycle, possibly within a pre-deltaic deposition environment.

4.1.4 Coal lithofacies

Coal is primarily composed of black coal seams or coal debris, which exhibits two main distribution states: continuous and stable or discontinuous unstable. The presence of coal indicates a relatively balances rate between the rise of base levels and peat accumulation, with minimal input of terrestrial clastic materials (Shao et al., 2017). The main coal seams developed in the study area are mainly distributed in the J_1b_1 and the J_2x_2 (Figure 1).

4.2 Based on the genesis sandbodies of fluvio-delta

Identifying different types of sandbodies is not only essential for clarifying the stacking patterns of sandbodies but also forms the basis for effective reservoir prediction. In this paper, we identify five types of genetically different sandbodies through comprehensive analysis of cores, lithofacies, and outcrop (Figure 3; Table 1).

4.2.1 Distributary channel sandbodies

It is mainly composed of reddish-brown medium-thick bedded sandstones, typically overlying debris flow, normal grain sequence, with normal grading and multiple sets of sandbodies stacked vertically. Lithofacies is mainly Sm. It belongs to near-source deposition under high energy conditions. The top and bottom of the sandstone are in abrupt contact with carbonaceous mudstone, conglomerate, or erosional surfaces. The sandbodies of this genetic type are mainly distributed in the J_1b_5, J_1b_3, and J_1b_1.

4.2.2 Subaqueous distributary channel sandbodies

These are submerged extensions of distributary channels after they enter the lake, primarily composed of gray-green and brown medium-bedded sandstones. They commonly exhibit combination of St, St, and Sh. The sandbodies of this genetic type are distributed in the Badaowan Formation.

4.2.3 Mouth bar sandbodies

These are mainly composed of gray-green medium-thin sandbodies, which are composed of single or multiple upwardly thickened sandbodies. Sp are commonly seen, with lateral migration being the main feature and high structural and composition maturity. The sandbodies of this genetic type are distributed in the Badaowan Formation.

4.2.4 Braided channel sandbodies

These are mainly composed of gray-green medium- to thick-bedded sandbodies, with St and Sp. The scouring-filling structures are developed, and variegated boulder clay can be observed at the bottom of the channel. Controlled by slope, provenance supply, and hydraulic energy, the sandbodies primarily migrate laterally. The sandbodies are braided and widely distributed on the plane. The genetic sandbodies are the skeleton sandbodies that constitute the braided river delta, and are also the reservoir sandbodies of the Xishanyao Formation.

10.3389/feart.2024.1503646

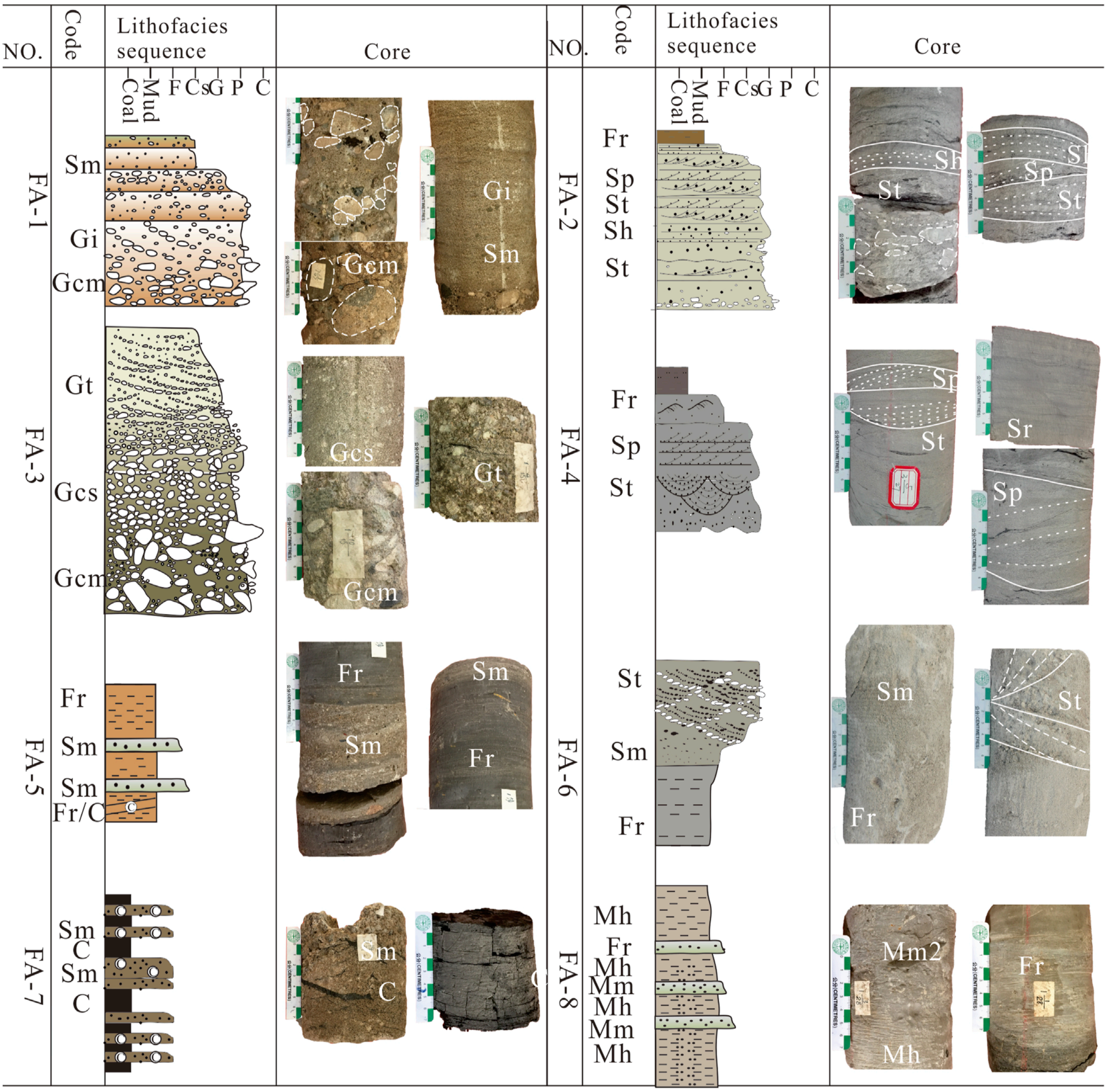

FIGURE 3
Genetic sandbodies sequence and characteristic of Fluvio-delta with coal-bearing strata of Middle-Lower Jurassic in Hongshanzui area in the Junggar Basin. FA-1 is distributary channel sandbodies. FA-2 and FA-3 are subaqueous distributary channel sandbodies. FA-4 is braided channel sandbodies. FA-5 is distributary bay. FA-6 is mouth bar sandbodies. FA-7 and FA-8 are overflow sandbodies.

TABLE 1 Types and distribution of genetic sandbodies with coal-bearing strata of Middle-Lower Jurassic in Hongshanzui area in Junggar Basin.

Sedimentary facies	Sedimentary subfacies	Genetic sand body type	Distribution layer
Fan delta	Fan delta plain	Distributary channel	J_1b_5, J_1b_3, and J_2b_1
	Fan delta front	Subaqueous distributary channel	J_1b_5, J_1b_4, J_1b_3, and J_1b_1
		Mouth bar	J_1b_5, J_1b_4, J_1b_3, and J_1b_1
Braided river delta	Braided river delta plain	Braided river channel	J_2x_1, J_2x_2, J_2x_3, and J_2x_4
		Overflow sand	J_2x_1, J_2x_2, J_2x_3, and J_2x_4

FIGURE 4
Coal of distribution with coal-bearing strata of Middle-Lower Jurassic in Hongshanzui area in the Junggar Basin. **(A)** Continuous and stable coal seams, developed in J_1b_1, located in northwestern margin of the Junggar Basin; **(B)** discontinuous and unstable coal seams, developed in J_2x_2, located in northwestern margin of the Junggar Basin; **(C)** continuous and stable coal seams of the J_1b_1 observed in the core; and **(D)** discontinuous and stable coal seams of the J_2x_2 observed in the core.

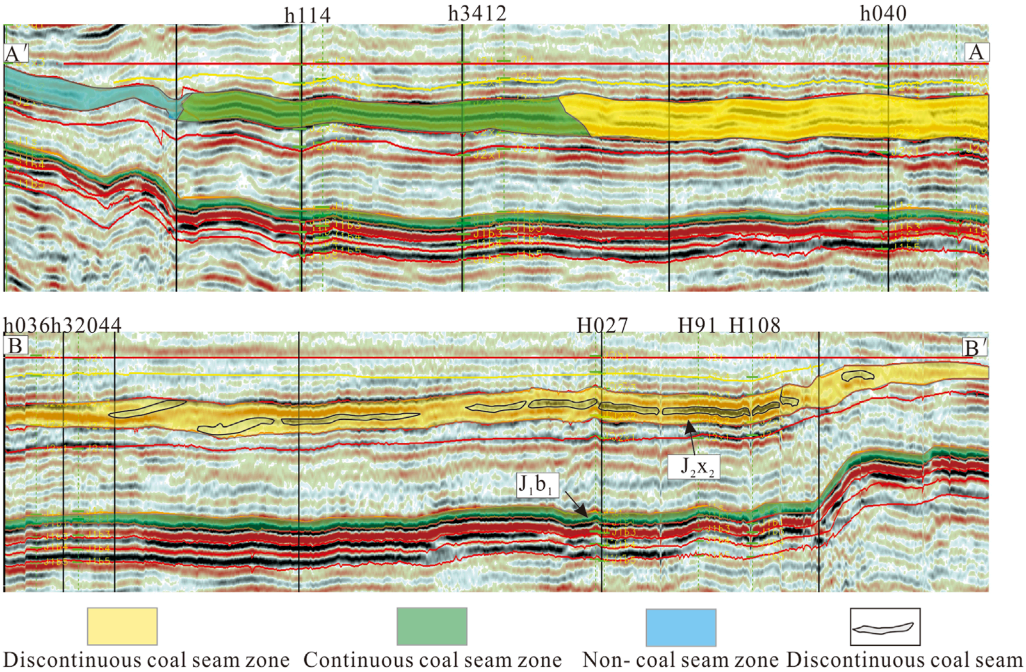

FIGURE 5
Seismic profiles with coal-bearing strata of Middle-Lower Jurassic in Hongshanzui area in the Junggar Basin. The seismic profiles **(AA′, BB′)** show that the subsidence amplitude is small, and the seismic in-phase axis is continuous. In the Xishanyao Formation, the seismic in-phase axis is discontinuous.

FIGURE 6
Characteristic of conglomerate with debris flow of well J356.

10.3389/feart.2024.1503646

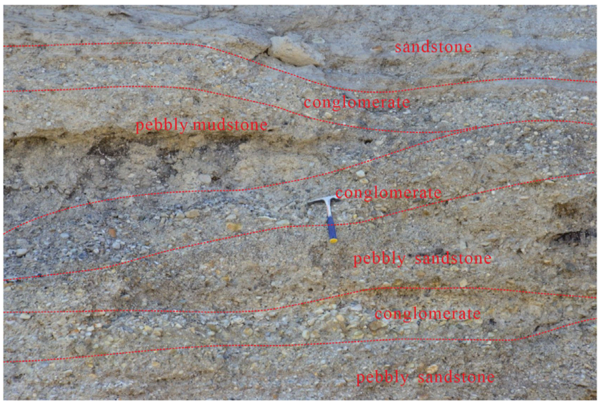

FIGURE 7
Conglomerate of Jurassic Badaowan Formation of Tuziakneigou in the Junggar Basin.

4.2.5 Overflow sandbodies

The Fr is developed and distributed around the braided channels. This type of sandbodies is distributed throughout the Xishanyao Formation.

4.3 Distribution characteristics of genesis sandbodies and coal seam

Based on the outcrops and core, the coal seams are mainly distributed in the J_1b_1 and the J_2x_2, but there are significant differences in thickness, continuity, and the superposition relationship with sandstone (Figure 4). Through core analysis, the J_1b_1 exhibits a set of thick, 1.3 m coal seams. Theses coal seams are predominantly sandwiched sandstones (Figure 4C). On seismic sections, they appear as continuous and stable strong amplitude isochronous. In contrast, the J_2x_2 contains several sets of thin coal seams, 0.1–0.5 m thick (Figure 4D). On seismic sections, these coal seams often manifest as discontinuous and unstable weak amplitude isochronous axis (Figure 5).

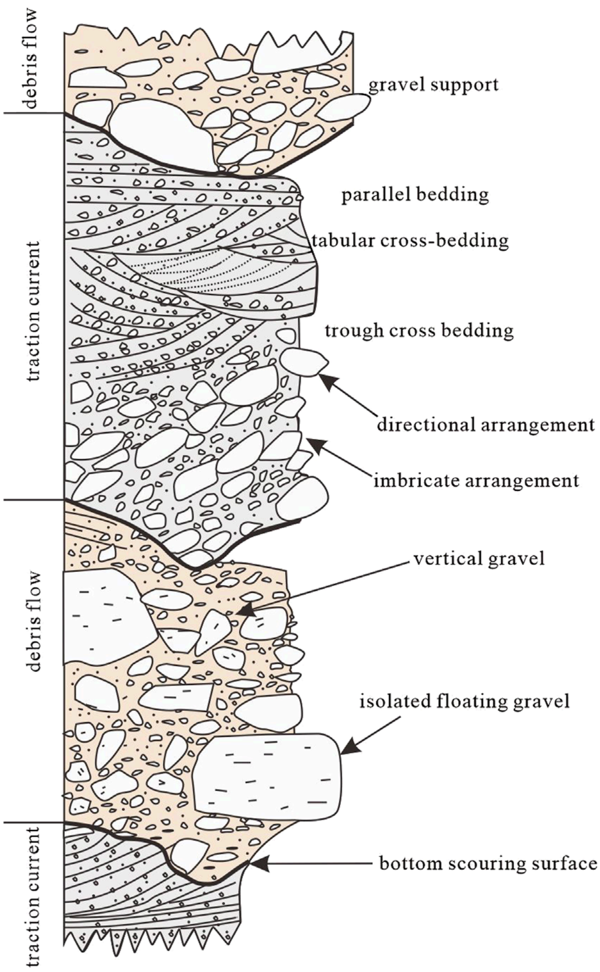

FIGURE 8
Sedimentary sequence with debris flow and traction current with coal-bearing strata of Middle-Lower Jurassic in Hongshanzui area in the Junggar Basin.

5 Discussion

5.1 Discussion on the genesis of sandbodies

In the classical sedimentological classifications, such as deltaic, sandstone, and carbonate sedimentary facies classifications, the genetic classification schemes are commonly employed. In this article, genetic classification approach is introduced into the classification of conglomerates, sandstones, and coal seams, and the implications of caused classification in the contexts are explored.

Based on the core observation, Lithofacies identification and transportation mechanisms were performed. Taking the sedimentary sequence of lithological characteristics, MPS/BTh, and grain size characteristics as the identification criteria, two types of genetic conglomerate developed in the study area have been effectively identified: debris flow genetic conglomerate and traction current genetic conglomerate. The genetic classification of conglomerate established in this study emphasizes on sedimentary genesis and has the characteristics of easy identification and strong operability.

5.1.1 Debris flow-induced conglomerate

5.1.1.1 Petrological characteristics

Debris flow is plastic sedimentary flow, characterized by linear laminar flow, and can be rich in sandstone or mudstone. Core samples from Well J356 and the outcrop of Tuziakneigou section show that the conglomerate caused by debris flow is usually reddish-brown, red, and grayish-brown, with a wide range of grain sizes, ranging from 80 mm to 2 mm. It is usually composed of massive conglomerate, with no contact between the gravels, poorly sorted grains of mixes sizes, moderate-to-poor roundness, and lack of sedimentary structures. Course gravel often "floats" with a matrix of finer grains, resulting in high matrix content. These conglomerates show abrupt contacts with underlying and overlying sandstones, indicating characteristics

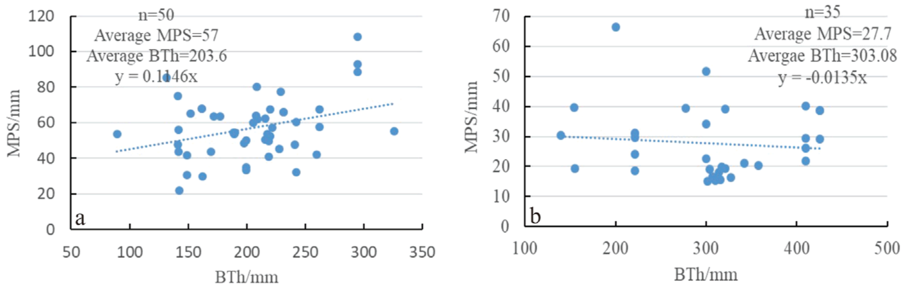

FIGURE 9
Distribution statistics of MPS/BTh with difference genetic conglomerate with coal-bearing strata of Middle-Lower Jurassic in Hongshanzui area in the Junggar Basin. **(A)** Debris flow. **(B)** Traction current.

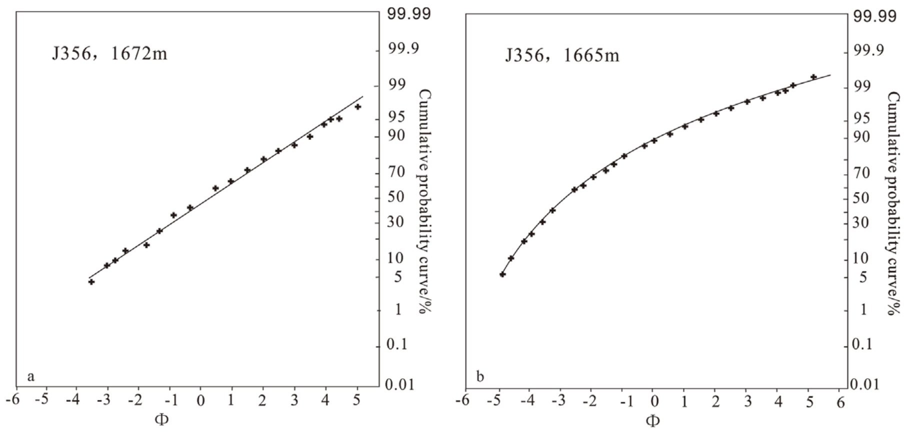

FIGURE 10
Cumulative probability curve of genetic conglomerate with debris flow of coal-bearing strata of Middle-Lower Jurassic in Hongshanzui area in the Junggar Basin. **(A)**. Linear. **(B)** Wide-gentle arch.

of sedimentary massive freezing and plastic flow deformation (Carter, 1975) (Figures 6, 7).

5.1.1.2 Sedimentary sequence

Sedimentary sequence with debris flow and traction current through core and outcrop observations (Figure 8): the conglomerate of the debris flow is mainly composed of cobble and pebble, and no obvious grain bedded vertically. The thickness of the single layer ranged from 40 to 90 cm, and Gcm and Gmm are often developed.

It indicates that the fan body forms a multi-stage gravel debris channel under the control of allocycles (it is the product of changes in A/S by sediment supply, tectonic subsidence, sea level, and climate, Read and Forsyth, 1989) and autocycles (it only controls the internal structure of sedimentary facies and proportion of various lithofacies, with an unclear relationship to changes in base level cycles) factors (Yin et al., 2017).

5.1.1.3 MPS/BTh

Porêbski (1981) first proposed using statistical analysis of conglomerate with MPS (maximum particle size) and thickness of single layer (BTh). The ratio relationship of MPS/BTh can reflect different sedimentary transport processes. Subsequently, Nemec et al. (1984) also carried out the classification of debris flows based on the interpretation result.

In this paper, we select 50 samples to measure their maximum particle diameter and single-layer thickness, using a ruler to take measurements, and record the values for MPS and BTh. The results show that the average MPS is 57 mm and the average BTh is 203.6 mm. The matching ratio of the MPS/BTh is 0.1146. It shows that the particles in the conglomerate are coarse, and the thickness of the single layer is small, which have characteristic of debris flow genesis (Figure 9A).

5.1.1.4 Cumulative probability curve of the sediments' granularity

The cumulative probability curve of the sediments' granularity is highly sensitive to hydrodynamic conditions. Referring to Visher (1969) for an understanding of typical cumulative probability curves in different sedimentary environments, according to the shape of the particle size probability cumulative curve (number of straight line segments, span, slope, *etc.*) in the study area, the grain size data of coring wells were analyzed by

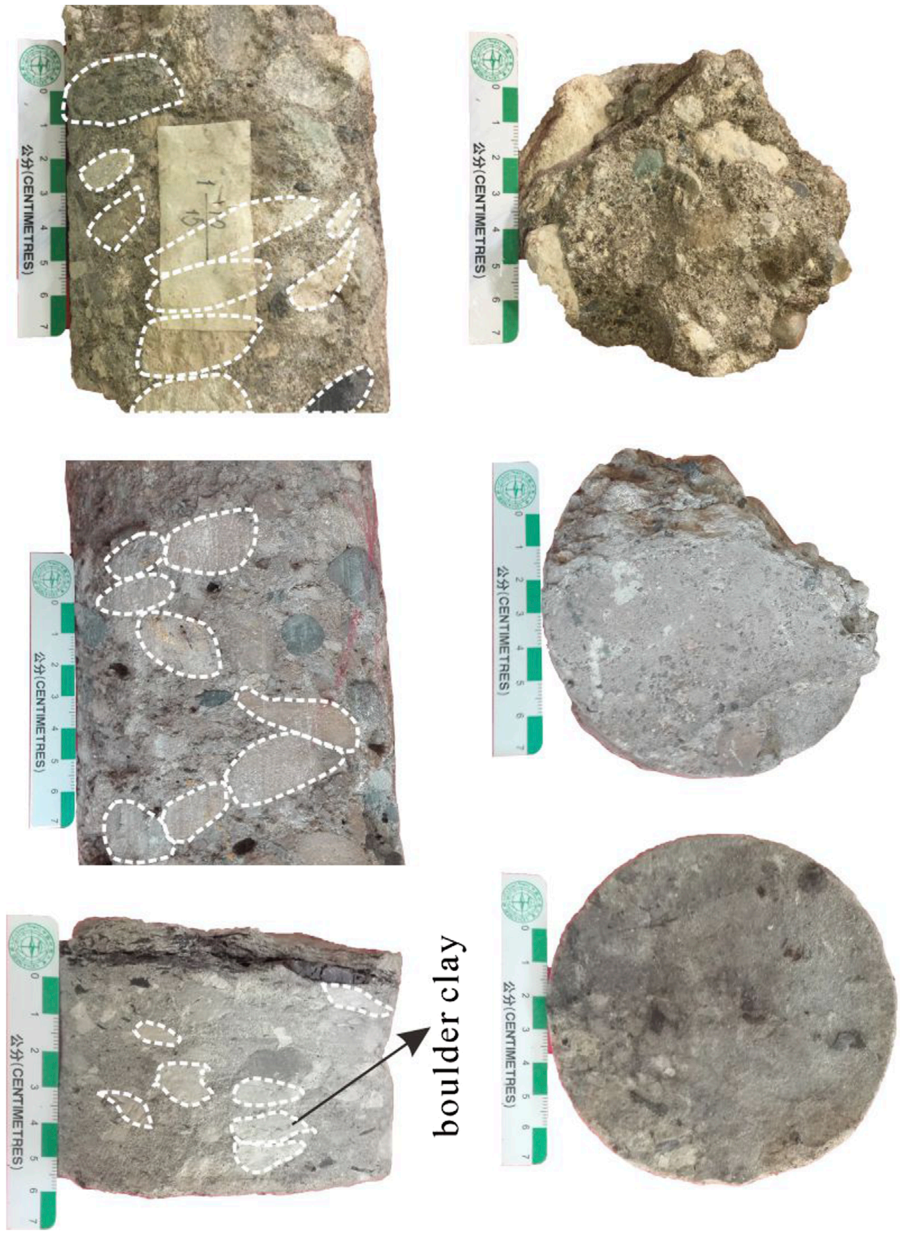

FIGURE 11
Characteristic of traction current of well HS2.

the sieving method, and the cumulative probability curve was plotted (Figure 10).

Debris flow genetic conglomerate can be classified into two types: linear type and wide-gentle arch based on their cumulative probability curve (Figure 10).

5.1.1.5 Linear

The curve is primarily exhibiting a single-segment straight line with a relatively gentle small slope (Figure 10A), with a total number of jumps between 5% and 95%, accounting for the majority of the entire particle size distribution. It reflects the general sorting and rapid accumulation of debris flow transporting methods, often characterized by Sm.

5.1.1.6 Wide-gentle arch

The overall differentiation of each subpopulation in the curve is not obvious and presenting slightly upward convex arc shape (Figure 10B). The particle size is relatively coarse with a wide distribution range, indicating poor sorting, where transported materials are predominated suspended, indicative of very high water medium energy. Vertically, the sediment grain size gradually becomes finer, arranged irregularly. This type of curve represents the distributary channel characterized by debris flow.

5.1.1.7 Depositional environment

The debris flows in the study area are triggered by gravity, exhibiting layering and transporting relatively large particles, with poorly

FIGURE 12
Genetic conglomerate outcrop with traction current of Dazhuluogou in the northeast of the Junggar Basin.

developed sedimentary structures. Gcm and Gmm are dominant, indicating a rapid mixed accumulation from a nearby land provenance. Early studies suggested that the debris flow is mostly distributed in the fan delta plain (Yao, 2018), further developing distributary channel in the J_1b_5 and at the bottom of the J_2x_1.

5.1.3 The genetic conglomerate formed by traction current

5.1.3.1 Petrological characteristics

The genetic conglomerate formed by traction flow is typically gray, with visible imbrication and oriented arrangement of clasts. The maturity of structure and composition in traction current is superior to those in debris flow conglomerates, with a lower matrix content, indicating that these conglomerates have been washed and transported over a certain distance (Figures 11, 12). This resulted in continued transport after collapse and deposition of overlying sediment, indicative of allochthonous sediment transport.

5.1.3.2 Sedimentary sequence

The genetic conglomerate formed by traction current is dominated by cobble and pebble, with significant single-layer thickness. Vertically, they exhibit either normal or inverse grading, often developing typical lithofacies sequences formed by traction current deposition, such as the Gcs, Gt, and Gi (Figures 2, 3). They typically develop in subaqueous distributary channel or mouth bar depositional environments (Yuan, 2016).

5.1.3.3 MPS/BTh

The average MPS in the study area is 27.7 mm, with an average BTh of 303.08, and the MPS/BTh is 0.0135 (Figure 9B), which reflects that the grain size of the conglomerate caused by the traction flow is finer than that of the debris flow, and their single-layer thickness is greater. This ratio can therefore serve as a criterion for identifying the conglomerate formed by traction flow.

5.1.3.4 Cumulative probability curve of traction current granularity

The cumulative probability curve of traction current granularity can also be divided into two categories: the low-slope two-jump one-hang three section type and the low-slope three section type.

5.1.3.5 The low-slope two-jump one-hang three section type

The grain-size distribution ranges from −2.5 to 5φ, which is composed of coarse and fine jump components, and the mass fraction of coarse jumping components is 5%–10%, with a coarse cutoff at -1φ. The mass fraction of fine jumping components is 10%–50%, and suspended components account for approximately 45% of the total mass, with a fine cutoff at 1.5φ (Figure 13A). The particle size probability cumulative curve shows significant variation in grain size, reflecting the strong hydrodynamic condition.

5.1.3.6 The low-slope three section type

This type of cumulative probability curve has a low slope, including low slope of 0.46, a low mass fraction (less than 5%), and a low mass fraction (5%–70%) of suspended subpopulation. The coarse cutoff is at −0.5φ and the fine cutoff is at 3φ (Figure 13B).

Both types of curves reflect the genesis of traction current deposition, and the sedimentary microfacies of underwater distributary channel and point bar with relatively low energy. This research finding is consistent with Tang et al. (2017) simulation of the sedimentary processes in shallow water fan delta development. It is considered that the fan delta plain is primarily composed of debris flow deposits, whereas the front is mainly dominated by traction current deposits formed by progradation processes.

5.1.3.7 Depositional environment

Traction currents exhibit numerous sedimentary structures such as Gcs, Gt, and Gi, which indicate underwater distributary channels. There are typically developed in the delta front within the study area.

By using the “four indicators” of structural-genetic conglomerate (petrological characteristics, sedimentary sequence, MPS/BTh, and cumulative probability curve), a semi-quantitative distinction between two types of genetic conglomerate is observed (Table 2).

Analyzing the classification of gravel based on structural-genesis and fluvial-deltaic sandstone facies revealed differences in sedimentary fluid properties and transport mechanisms within the study area. Debris flows, characterized by their coarse grain size, thin thickness, and high matrix content, are often used to indicate rapid deposition environments in delta plains. In contrast, traction currents have finer grain sizes, greater thickness, and well-developed layering, influenced by the washing and transport effects of water flow, resulting in lower matrix content. Their stable hydrodynamic conditions facilitate the formation of sedimentary structures, making them a common criterion for assessing delta front environments. These facies analysis aids in reconstructing the paleoenvironment, enhancing our understanding of the depositional history and the processes that shaped the region.

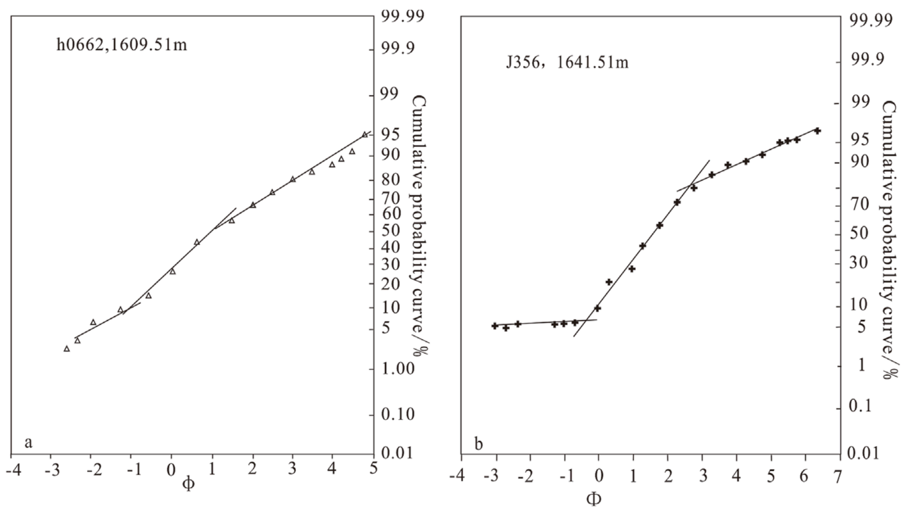

FIGURE 13
Cumulative probability curve of traction current granularity with coal-bearing strata of Middle-Lower Jurassic in Hongshanzui area in the Junggar Basin. **(A)** Low-oblique two-jump one-suspension three-stage type. **(B)** Low-oblique three-stage type.

TABLE 2 Difference between debris flow and traction current of genetic conglomerate with coal-bearing strata of Middle-Lower in Hongshanzui area in Junggar Basin.

Genetic conglomerate	Petrological characteristics	Sedimentary sequence	MPS/BTh	Granularity probability cumulative curve	Depositional environment
Debris flow	①Reddish brown, red ②Large particle size variation (2–80 mm) ③Low maturity in structure and composition ④Rich sand/mud, floating conglomerates, and high matrix content	Lack of sedimentary structures, dominated by Gcm and Gmm	0.1146	Linear; wide-gentle arch	Delta plain
Traction current	①Gray ②Small change in grain size ③High maturity in structure and composition ④Low matrix content	Development of sedimentary structures, dominated by Gcs, Gt, and Gi	0.0135	The low-slope two-jump one-hang three section type; the low-slope three section type	Delta front

5.2 Sedimentary genesis of coal seam

5.2.1 Tectonic

The coal-accumulating environment and coal-bearing structure of Jurassic in the Junggar Basin shows the diversity and particularity of Continental basins (Si, 2011). From the J_1b_5, the lake basin was in an expansion period, and gradually stabilizing toward a transitional phase by J_1b_1 (Li, 2007), with minimal climate fluctuations (He et al., 2016) (Figure 4C, Figure 6, Figure 7). Seismic sections (Figures 5AA′, BB′) indicate low subsidence rates. Genetic sandbodies are poorly developed, conducive to the formation of continuous and stable coal seams (Figure 5). During the period of the Sangonghe Formation, the lake basin officially entered the transitional stage, and a large set of extremely thick mudstone was developed, which were unfavorable for the development of coal seams. During the Xishanyao Formation period, the lake basin began to shrink and the delta system began to resurrect, resulting in turbulent water bodies, forming multiple sets of thin and intermittent coal seams in the J_2x_2 (Figure 4D, Figure 14).

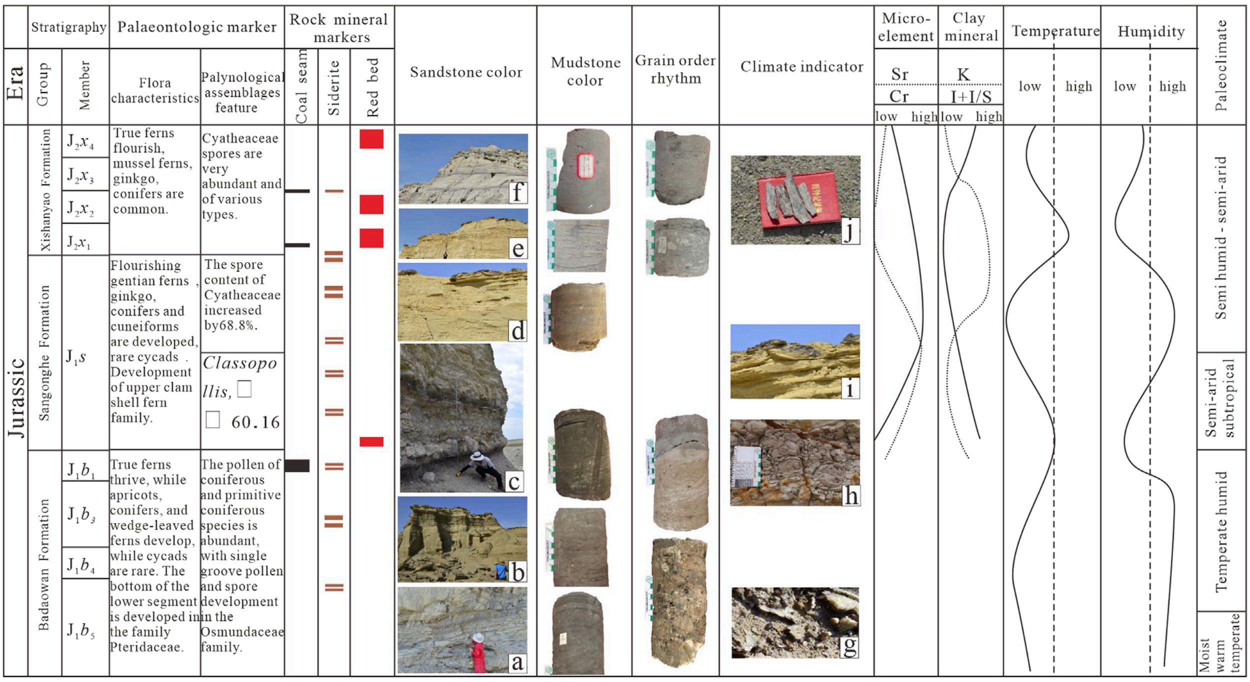

FIGURE 14
Paleoclimate of Middle-Lower Jurassic in Hongshanzui area in the Junggar Basin (The content of trance element, minerals, temperature, and humidity data are modified by Xinjiang Oilfield Exploration and Development Research Institute, 2001.). From the J1b to the J2x, the climate indicator changes. Paleontology: during the early Jurassic Badaowan Formation, the plant communities of true ferns, apricots, conifers, and double fans were abundant in coniferous pollen, and sporopollenin assemblages such as single groove pollen and spores of the Osmundaceae family developed; during the Middle Jurassic period of the J2x, true ferns and ginkgoes were common, and the spores of the Cyatheaceae family were very abundant and diverse in types. Mud color: the color of the mudstone has undergone a process of gray-black→ reddish-brown→ gray-white from the J1b to the J2x. Grain order rhythm: gravel→ mud→ coal→ sand→ coal→ mud. Paleosalinity experienced changes from low to high and then to low, and the change of K element has experienced a process from low mutation to high and then gradually lower. **(A)** Gray conglomerate; **(B)** Light yellow sandy mudstone; **(C)** Gray gravelly sandstone; **(D)** Light yellow sandstone; **(E)** Light yellow muddy sandstone; **(F)** Gray-white coal-bearing sandstone; **(G)** gypsum crystals; **(H)** spheroidal weathering; **(I)** Light yellow muddy sandstone; **(J)** Petrified wood.

5.2.2 Paleoclimate

In the continental setting, climate change has undoubtedly become the most important influencing factor (Maddy, 2016), especially for the sedimentary evolution of the Junggar Basin (Khadkikar et al., 1999; Vandenberghe, 2003; Mader and Redfern, 2011). The influence of climate change on the genesis of sandbodies and coal seams is illustrated by the changes of paleontological indicators, rock and mineral indicators, mudstone color, grain size rhythm, climate indicators, trace elements, clay minerals, temperature, and humidity (Figure 14). In the sedimentary sequence of ancient continent, the influence of climate on deposition has focused on the identification and analysis of ancient soil (Atchley et al., 2004; Cleveland et al., 2007; Ruskin and Jordan, 2007; Opluštil et al., 2015). Special minerals play an important role in climate indicators (Dalman et al., 2015; Mees, 2015). The trace elements contained in sedimentary rocks are indicative of climate and paleoenvironment (Curtis, 1990; Roy et al., 2010; Yang et al., 2016). Chemical alteration on land is influenced by climate and temperature, and warm climate contributes to chemical alteration. Sr element reflects the change of paleosalinity (Gao et al., 2015). The change of potassium content reflects the degree of chemical alteration (Nesbitt Amp and Young, 1982; Yang et al., 2006); the higher the potassium content, the stronger the chemical alteration, reflecting the more humid and hotter climate, and *vice versa*.

According to the literature data of the Exploration and Development Research Institute of Xinjiang Oilfield Company (2001) and He et al. (2016), the fluctuation of temperature and humidity from the J_1b to the J_2x was revealed. From the J_1b_5 to the J_1b_1, the temperature gradually increases from low to high, and the climate changes from warm temperate humid to temperate humid, which is conducive to the development of coal seams. The overall temperature of the J_2x fluctuates greatly and continues to decline, which provides favorable conditions for the development of coal seams. At the end of the period, the temperature rebounded and the development of coal seams has gradually stopped.

During the whole Badaowan Formation period, the humidity in the study area was relatively high, and it began to decrease at the top. With the change of humidity, the gravely sandstone gradually decreased, and the coal seams began to develop. During the period of the J_2x, the humidity was lower than that of the Badaowan Formation, but it still showed a rising trend. The bottom of the J_2x humidity was relatively high, and it was speculated that the hydrodynamic forces was strong, and the boulder clay was deposited. With the increase of

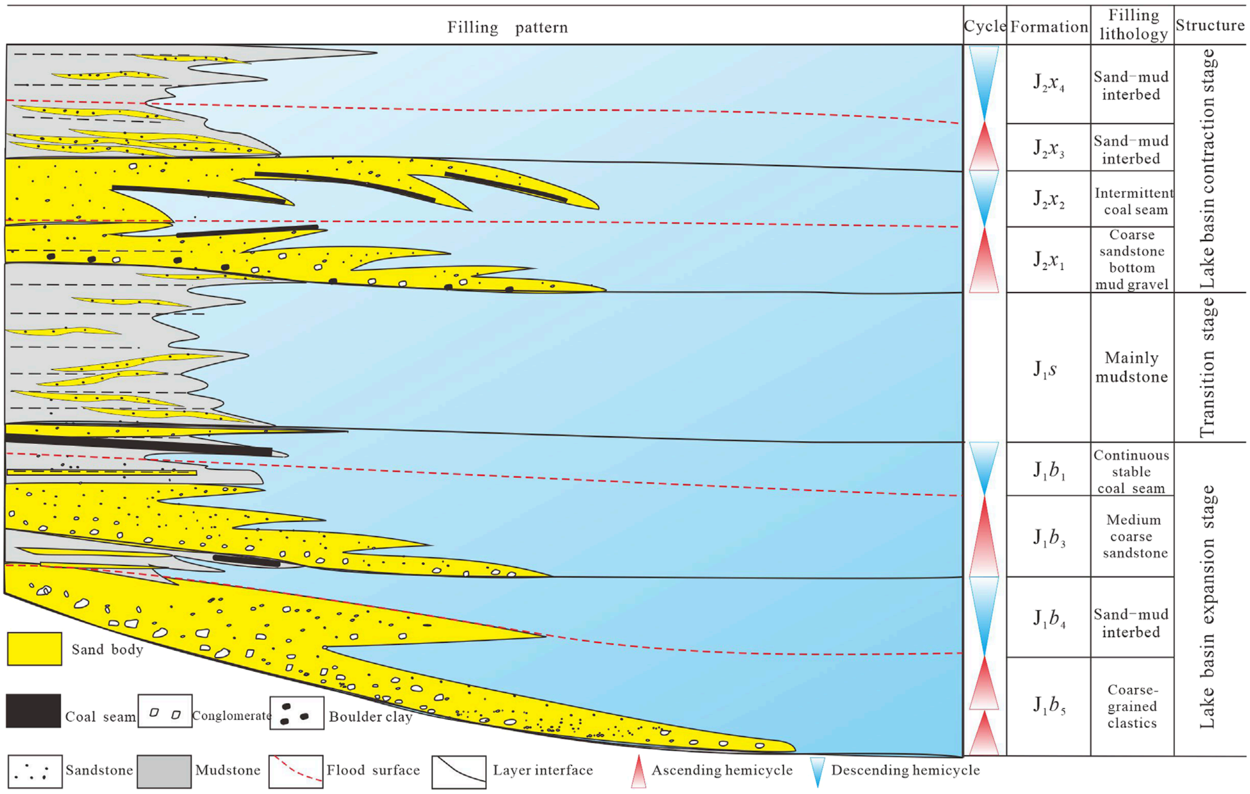

FIGURE 15
Filling model with coal-bearing strata of Middle-lower Jurassic in Hongshanzui area in Junggar Basin.

humidity, the conditions for coal seam development were reached, and multiple sets of intermittent coal seams were deposited in the middle of the J_2x.

Through the analysis of the characteristics of the above climatic indicators, it was fully proven that from the J_1b to the J_2x, the paleoclimate mainly experienced change from warm temperate humid→ temperate humid→ subtropical semi-arid→ semi-humid semi-arid. The change of climate is the formation of thick and stable continuous distribution of coal seam in the J_1b_1, and the formation of multiple sets of thin and intermittent unstable distribution of coal seam in the J_1x_2.

5.2.3 Sedimentary environment

The influence of depositional environments on the formation of coal seams and sandbodies mainly manifests in the depositional materials formed in thesis environments, providing the framework for the deposition of peat or coal, thereby affecting the formation and distribution of peat (Shao et al., 2017).

During the period of the Badaowan Formation, the fan delta was developed, characterized by the terrestrial clastic system. Subsequently, due to the slow rise of the base level, the delta plain began to transform into peat swamps and a set of continuous stable coal seam was formed in the J_1b_1 (Figure 14). During this period, the accumulation rate of peat remained consistent with the tectonic subsidence rate for a long time. Coal accumulation process lasted for a long time with high intensity and a wide distribution. As the lake continued to retreat, the base level dropped too rapidly, leading to a state of under-compensation in mudstone deposition that was unfavorable for plant growth. This caused a gradual weakening of coal accumulation. A set of thin-layer fine sandstone or coarser gravel sandstone is formed on the roof and floor of the coal seam (Figure 14).

During the period of the Sangonghe Formation, the appearance of thick mudstone indicates it was a lake basin period unsuitable for coal accumulation. Starting from the J_2x_1, the climate gradually became dry and hot, causing intermittent exposure of sedimentary interfaces. The lake basin began to transform into a swamp, whereas the delta system became resurrected, and coal lines began to appear locally. Scattered carbonaceous bands were visible in the core samples (Figure 14). According to (Zhu et al., 2004) the model of lake basin swamping and coal accumulation stage, multiple sets of coal seams developed in the J_2x_2, each corresponding to a stage of lake basin swampification. During this period, the short-term climate fluctuation temporarily halted swampification, and the gravel was filled, thus forming multiple sets of discontinuous coal seams. The cross-section of provenance seismic profile (AA') shows that the coal seams are discontinuously distributed. The profile along the provenance (BB') demonstrates discontinuous coal seams developed in areas with topographic fluctuation, whereas continuous coal seams form in gentle sloping areas, with uplifted zone devoid of coal seams (Figure 14). Core samples indicate interbedded sedimentation between coal seams and sandstone. To the J_2x_3, due to persistent dry and hot climate, and rapid rise of the base level, the equilibrium state was disrupted, with coal seams only persisting in localized areas.

From the perspective of sedimentary facies, coal seams are primarily distributed in three environments: interdistributary bay, swamp environment, and partly within the subaqueous interdistributary bay. In braided river delta plains, coal seams are mainly distributed in the peat swamp environment formed after the gradual abandonment of the braided channels (Yao, 2018).

6 Sedimentary filling model

Based on the analysis, during the Badaowan Formation period, the northwestern margin of Junggar experienced a warm temperate humid to temperate humid climate. This climate was characterized by weak monsoons, relatively subdued wave activity, and minimal coastal currents. Such conditions favored the formation of debris flow and traction flow genesis conglomerates, as well as underwater distributary channel sandbodies and the estuary bar. Horizontally, the grain size of the sand body from the west to the east becomes finer, and their thickness also diminishes. During the ascending phase of the sedimentary cycle, sandbodies generally retreat toward the source area. Conversely, in the descending half cycle, these sandbodies advance toward the basin. The strata along the source section are relatively flat, and continuous and stable set of coal seams has developed within in the $J_1b_{1.}$

During the Xishanyao Formation period, the climate was relatively mild and dry, with strong monsoon activity that led to the washing and reformation of sandbodies. This was characterized by small-scale development of traction flow conglomerate, braided channel sand body development, as well as the formation of multiple sets of thin-layer, intermittent, and unstable coal seams. Notably, the number of developed coal seams decreased as one approached the denudation area (Figure 15). Vertically, from the J_1b_5 to the J_2x_4, there is a gradual fining of particle size and an increase in the argillaceous interlayer. The sandbodies deposited during the rising phase of the sedimentary cycle are thicker than those deposited during the falling phase, with the main coal seams primarily during the falling phase.

7 Conclusion

1) On the basis of fine core observation, five types of conglomerate facies are identified: Gcs, Gcm, Gmm, Gt, and Gi, and five kinds of sandstone facies are identified: Sm, Sp, St, Sh, and Fr. Two kinds of mudstone facies are identified: Mh and Mm, and one coal phase, C.
2) Four indexes for semi-quantitative identification of structural-genetic conglomerates are proposed: petrological characteristics, sedimentary sequence, maximum particle size/single layer thickness (MPS/BTh), and grain size probability accumulation curve. These effectively distinguish two types of genetic conglomerate (debris flow and traction flow). Additionally, the genesis of four sandbodies types—distributary channel, underwater distributary channel, estuary bar, and overflow—has been clarified based on river delta genesis.
3) A comprehensive analysis of structure, paleoclimate, sedimentary environment, and coal seam genesis mechanism reveals that during the J_1b_1, stable structural conditions, limited subsidence, a temperate humid climate, and the minimal climate fluctuation led to the formation of a thick, continuous, and stable coal seam distribution in the interdistributary bay and swamp environment of the fan delta plain. In contrast, during the period of the J_2x_2, fluctuating strata, variable climate conditions, and unstable source supply resulted in multiple sets of thin and intermittently distributed coal seams within the swamp environment.

Data availability statement

The original contributions presented in the study are included in the article/Supplementary Material; further inquiries can be directed to the corresponding author.

Author contributions

YZ: writing–original draft and writing–review and editing. WW: software and writing–review and editing. WY: supervision and writing–original draft. XZ: validation and writing–review and editing. YX: data curation, resources, and writing–review and editing. YF: visualization and writing–review and editing. ZQ: formal analysis and writing–review and editing.

Funding

The author(s) declare that financial support was received for the research, authorship, and/or publication of this article. This study was supported by the Tianshan Talent Training Program (2023TSYCCX0002) and the National Natural Science Foundation of China (No. 41902109).

Acknowledgments

This study received aid from the research team at the Xinjiang University. Additionally, the authors thank all of the field assistants, who offered invaluable support to this study.

Conflict of interest

Author WY was employed by SINOPEC Shengli Oilfield Company.

Authors XZ and YX were employed by Xinjiang Oilfield Company.

Author YF was employed by PetroChina.

The remaining authors declare that the research was conducted in the absence of any commercial or financial relationships that could be construed as a potential conflict of interest.

Generative AI statement

The author(s) declare that no Generative AI was used in the creation of this manuscript.

Publisher's note

All claims expressed in this article are solely those of the authors and do not necessarily represent those of their affiliated organizations, or those of the publisher, the editors, and the reviewers. Any product that may be evaluated in this article, or claim that may be made by its manufacturer, is not guaranteed or endorsed by the publisher.

References

Afterward, H. M. (1972). The role of subaqueous debris flow in generating turbidity currents. *Jour. Sediment. Petrol.* 42, 775–793. doi:10.1306/74D710C5-2B21-11D7-8648000102C1865D

Allen, J. R. L. (1982). *Sedimentary structures their character and physical basis*, 1. Elsevier scientific Publishing Co.

Allen, J. R. L. (1983). Studies in fluviatile sedimentation: bars, bar-complexes and sandstone sheets (low-sinuosity braided streams) in the brownstones (L. devonian), Welsh borders. *Sediment. Geol.* 33, 237–293. doi:10.1016/0037-0738(83)90076-3

Allen, P. A., Michael, N. A., Arcy, M. D., Roda-Boluda, D. C., Whittaker, A. C., Duller, R. A., et al. (2016). Fractionation of grain size in terrestrial sediment routing systems. *Basin Res.* 29, 180–202. doi:10.1111/bre.12172

Atchley, S. C., Nordt, L. C., and Dworkin, S. I. (2004). Eustatic Control on Alluvial Sequence Stratigraphy: A Possible Example from the Cretaceous-Tertiary Transition of the Tornillo Basin, Big Bend National Park, West Texas, U.S.A. *J. Sediment. Res.* 74, 391–404. doi:10.1306/102203740391

Cao, Y. Z., Yang, T., Wang, Y. Z., Wang, Y. Z., Zhang, S. M., Wang, S. J., et al. (2017). Types and genesis of deep-water hybrid event beds comprising debris flow and turbidity current. *Earth Sci. Front.* 24, 234–248. doi:10.13745/j.esf.2017.03.234

Cleveland, D. M., Atchley, S. C., and Nordt, L. C. (2007). Continental Sequence Stratigraphy of the Upper Triassic (Norian Rhaetian) Chinle Strata, Northern New Mexico, U.S.A.: Allocyclic and Autocyclic Origins of Paleosol-Bearing Alluvial Successions. *J. Sediment. Res.* 77, 909–924. doi:10.2110/jsr.2007.082

Curtis, C. D. (1990). Aspects of climatic influence on the clay mineralogy and geochemistry of soils, palaeosols and clastic sedimentary rocks. *J. Geol. Soc. Lond.* 147, 351–357. doi:10.1144/gsjgs.147.2.0351

Dalman, R., Weltje, G. J., and Karamitopoulos, P. (2015). High-resolution sequence stratigraphy of fluvio–deltaic systems: Prospects of system-wide chronostratigraphic correlation. *Earth Planet. Sci. Lett.* 412, 10–17. doi:10.1016/j.epsl.2014.12.030

Diessel, C., Boyd, R., Wadsworth, J., Leckie, D., and Chalmers, G. (2000). On balanced and unbalanced accommodation/peat accumulation ratios in the Cretaceous coals from Gates Formation, Western Canada, and their sequence-stratigraphic significance. *Int. J. Coal Geol.* 43, 143–186. doi:10.1016/s0166-5162(99)00058-0

Gao, M., Yang, M., Lu, Y., Levin, V. A., He, P., and Zhu, H. (2024). Mechanical characterization of uniaxial compression associated with lamination angles in shale. *Adv. Geo-Energy Res.* 13 (1), 56–68. doi:10.46690/ager.2024.07.07

Gao, Z. Y., Zhou, C. M., Feng, J. R., Cui, J. G., Guo, M. L., and Wu, H. (2015). Distribution of a large area of sand body Formation Mechanism: Ephemeral Straeams in Arid Climate. *Acta Sedimentol. Sin.* 33, 427–438. doi:10.13962/j.issn.1000-0550.2015.03.011

Georgiopoulou, A., Masson, D. G., Wynn, R. B., and Krastel, S.(2013). Sahara Slide: Age, initiation, and processes of a giant submarine slide. *Geochem. Geophy. Geosy.* 11, 1–22. doi:10.1002/ggge.20078

He, Z. B., Liu, Z. Y., Yang, Y., Guo, Q., Song, J. Y., and Ji, H. L. (2016). Discussion on the relationship between Cenozoic tectonic-sedimentary evolution and sandstone-type uranium mineralization in the Junggar Basin. *Xinjiang Geol.* 34, 410–417. doi:10.3969/j.issn.1000-8849.2016.03.010

Hemmesch, N. T., Harris, N. B., Mnich, C. A., and Selby, D. (2014). A sequence-stratigraphic framework for the Upper Devonian Woodford Shale, Permian Basin, west Texas. AAPG *Bulletin. Am. Assoc. Pet. Geol. Bull.* 98, 23–47. doi:10.1306/05221312077

Hu, Z. Q., and Li, M. J. (2003). Sequence modeling and sedementary facies evolution of Jurassic in northwestern edge of Junggar Basin. *Oil Gas. Geol.* 24, 351–355. doi:10.3969/j.issn.1000-8227.2003.04.007

Hu, Z., and Zhu, X. (2002). *Diageneses and pose evolution of Jurassic reservoir in northwestern edge of Junggar basin [J]. Journal of the University of Petroleum* 26 (3), 16–19.

Johnson, A. M. (1965). A Model for Debris Flow. *Geol. Soc. Am. Bull.* 76, 791–800.

Khadkikar, A. S., Mathew, G., Malik, J. N., Gundu Rao, T., Chowgaonkar, M., and Merh, S. (1999). The influence of the South-west Indian monsoon on continental deposition over the past 130 kyr, Gujarat, western India. *Terra nova.* 11, 273–277. doi:10.1046/j.1365-3121.1999.00258.x00252.x

Li, W. (2007). Li Wei. Mesozoic basin formation mechanism and tectonic evolution of orogenic belt in northwestern junggar. *China Acad. Geol. Sci.* 2007 PhD thesis.

Li, X. B., Liu, H. Q., Zhang, Z. Y., Yuan, X. Q., Wan, Y. R., Niu, H. Q., et al. (2014). "Argillaceous parcel" structure: Adirect evidenceof debris flow orgin of deep-water massive sandstone of Yanchang Formation, Upper Triassice, the Ordos Basin. *Acta Sedimentol. Sin.* 32, 611–622. doi:10.3969/j.issn.1000-0550.2014.04.009

Liu, G., Wei, Y. Z., Chen, W., Gong, D. Y., Wang, F., Sun, J., et al. (2018). Sand-body structura and reservoir forming control of Jurassic Sangonghe formation in well block shinan 13, Luxi area, Junggar Basin. *Acta Pet. Sin.* 39, 1006–1018. doi:10.8117/j.issn.0498-160X.2018.09.001

Carter, R. M. (1975). A discussion and classification of subaqueous mass-transport with particular application to grain-flow, slurry-flow, and fluxoturbidites. *Earth Sci. Front.* 11, 145–177. doi:10.1016/0012-8252(75)90098-7

Maddy, D. (2016). An evaluation of climate, crustal movement and base level controls on the Middle-Late Pleistocene development of the River Severn, U.K. *U.K. Neth. J. Geosci.* 81, 329–338. doi:10.1017/s0016774600022630

Mader, N. K., and Redfern, J. (2011). A sedimentological model for the continental Upper Triassic Tadrart Ouadou Sandstone Member: recording an interplay of climate and tectonics (Argana Valley; South-west Morocco). *Sedimentology* 58, 1247–1282. doi:10.1111/j.1365-3091.2010.01204.x

Mees, F. (2015). Distribution patterns of gypsum and kalistrontite in a dry lake basin of the southwestern Kalahari (Omongwa pan, Namibia). *Earth Surf. Process. Landforms* 24, 731–744. doi:10.1002/(sici)1096-9837(199908)24:8<731::aid-esp7>3.0.co;2-0

Meng, J. F., Guo, Z. J., and Fang, S. H. (2009). A new insight into the thrust structures at the northwestern margin of Junggar Basin. *Earth Sci. Front.* 16, 171–180. doi:10.1360/02-2009-3-2-171

Middleton, G. V., and Hampton, M. (1976). Subaqueous sediment transport and deposition by sediment gravity waves. *AAPG Bull.* 60, 115–120. doi:10.1306/703B3D03-1707-11D7-8645000102C1865D

Nemec, W., Steel, R. J., Poreebski, S. J., and Spinnangr, A. (1984). Domba Conglomerate, Devonian, Norway: process and lateral variability in a mass flow-dominated, lacustrine fan-delta. *Geol. Quart.* doi:10.1111/j.1365-3091.1984.tb01157.x

Nesbitt Amp, H. W., and Young, G. M. (1982). Early proterozoic climates and plate motions inferred from major element chemistry of lutites. *Nature* 299, 715–717. doi:10.1038/299715a0

Opluštil, S., Lojka, R., Rosenau, N. A., Strnad, L., and Sýkorová, I. (2015). Middle Moscovian climate of eastern equatorial Pangea recorded in paleosols and fluvial architecture. *Palaeogeogr. Palaeocl.* 440, 328–352. doi:10.1016/j.palaeo.2015.09.009

Pei, Y., He, Y. B., Li, H., and Xiao, B. (2015). Discuess about Relationship between High-density Turbidity Current and Sandy Debris Flow. *Geol. Rev.* 61, 1281–1292. doi:10.3969/j.issn.0454-5659.2015.06.009

Porêbski, S. J. (1981). Ẃiebodzice Succession (Upper Devonian-Lower Carboniferous; Western Sudeten): A prograding, mass flow dominated fan-delta complex. *Geol. Quart.* 16, 101–192.

Postma, G. (1990). An analysis of the variation in delta architecture. *Terra nova.* 2, 124–130. doi:10.1111/j.1365-3121.1990.tb00052.x1990.tb00187.x

Read, W. A., and Forsyth, I. H. (1989). Allocycles and autocycles in the upper part of the limestone coal group (pendleian e1) in the glasgow–stirling region of the midland valley of scotland. *Geol. J.* 24 (2), 121–137. doi:10.1002/gj.3350240205

Roy, P. D., Caballero, M., Lozano, R., Ortega, B., Lozano, S., Pi, T., et al. (2010). Geochemical record of Late Quaternary paleoclimate from lacustrine sediments of paleo-lake San Felipe, western Sonora Desert, Mexico. *J. S. Am. Earth Sci.* 29, 586–596. doi:10.1016/j.jsames.2009.11.009

Ruskin, B. G., and Jordan, T. E. (2007). Climate Change Across Continental Sequence Boundaries: Paleopedology and Lithofacies of Iglesia Basin, Northwestern Argentina. *J. Sediment. Res.* 77, 661–679. doi:10.2110/jsr.2007.069

Shanmugam, G. (2000). 50 years of the turbidite paradigm (1950s—1990s): deep-water processes and facies models—a critical perspective. *Mar. Pet. Geol.* 17, 285–342. doi:10.1016/s0264-8172(99)00011-2

Shao, L., Wang, X., Lu, J., Wang, D. D., and Hou, H. H. (2017). A reappraisal on Development and Prospect of Coal Sedomentology in China. *Acta Sedimentol. Sin.* 35, 1016–1031. doi:10.14027/j.issn.1000-0550.2017.080

Si, M. N. (2011). *Characteristics and controlling factors of jurassic coal-bearing reservoirs in inner Junggar Basin*. Beijing: China university of petroleum.

Soltan, R., and Mountney, N. P. (2016). Interpreting complex fluvial channel and barform architecture: Carboniferous Central Pennine Province, northern England. *Sed* 63, 207–252. doi:10.1111/sed.12224

Sui, F. G. (2015). Tectonic Evolution and Its Relationship with Hydrocarbon Accumulation in the Northwest Margin of Junggar Basin. *Acta Geol. Sin.* 89, 779–793. doi:10.13545/j.jr.2015.04.002

Tan, C., Yu, X., Liu, B., Qu, J., Zhang, L., and Huang, D. (2017). Conglomerate categories in coarse-grained deltas and their controls on hydrocarbon reservoir distribution: a case study of the Triassic Baikouquan Formation, Mahu Depression, NW China. *Petgeo* 23, 403–414. doi:10.1144/petgeo2016-017

Tang, Y., Yin, T. J., Tan, J. H., and Wang, D. D. (2017). Development of Large-Scale Shallow-Water Fan Delta: Sedimentary Laboratory Simulation and Experiments. *Xinjiang Petrol. Geol.* 38, 253–263. doi:10.3969/j.issn.1001-5518.2017.03.007

Vandenberghe, J. (2003). Climate forcing of fluvial system development: an evolution of ideas. *Quat. Sci. Rev.* 22, 2053–2060. doi:10.1016/s0277-3791(03)00213-0

Visher, G. S. (1969). Grain size distributions and depositional processes. *J. Sediment. Res.* 39, 1074–1106. doi:10.1306/74D710E4-2B21-11D7-8648000102C1865D

Wang, S., Shao, L., Wang, D., Sun, Q., Sun, B., and Lu, J. (2019). Sequence stratigraphy and coal accumulation of Lower Cretaceous coal-bearing series in Erlian Basin, northeastern China. *AAPG Bull.* 103, 1653–1690. doi:10.1306/11211817175

Talling, P. J., Wynn, R. B., Masson, D. G., Frenz, M., Cronin, B. T., Schiebel, R., et al. (2007). Onset of submarine debris flow deposition far from original giant landslide. *Nature* 22 (450(7169)), 541–4. doi:10.1038/nature06313

Xian, B. Z., An, S. Q., and Shi, W. H. (2014). Subaqueous Debris Flow: Hotspots and Advances of Deep-water Sedimention. *Geol. Rev.* 60, 39–51. doi:10.3969/j.issn.0454-5659.2014.01.005

Xian, B. Z., Wan, J. F., Dong, Y. L., Ma, Q., and Zhang, J. G. (2013). Sedimentary characteristics, origin and model of lacustrine deep-water massive sandstone: An example from Dongying Formation in Nanpu depression. *Acta Pet. Sin.* 29, 3287–3299. doi:10.3976/j.issn.1000-0569.2013.09.012

Yang, S., Li, C., and Cai, J. (2006). Geochemical compositions of core sediments in eastern China: Implication for Late Cenozoic palaeoenvironmental changes[J]. *Palaeogeogr. Palaeoclimatol. Palaeoecol.* 229 (4), , 287–302.

Yang, T., Cao, Y. Z., Wang, Y. Z., and Zhang, S. M. (2015). Types, sedimentary characteristices and genetic mechanisms of deep-water gravity flows: a case study of the middle submember in Member 3 of Shahejie Formation in Jiyang depression. *Acta Pet. Sin.* 9, 1048–1059. doi:10.7623/syxb201509011

Yang, Y., Fang, X., Koutsodendris, A., Ye, C., Yang, R., Zhang, W., et al. (2016). Exploring Quaternary paleolake evolution and climate change in the western Qaidam Basin based on the bulk carbonate geochemistry of lake sediments. *Palaeogeogr. Palaeocl.* 446, 152–161. doi:10.1016/j.palaeo.2016.01.021

Yao, Z. Q. (2018). *The sedimentogenesis and reservoir characterization with coal measures of middle-lower jurassic in Hongshanzui area of Junggar Basin*. Beijing: China University of Geosciences.

Yao, Z. Q., Yu, X. H., Deleqiati, J. N. T. I., Huang, D. J., Tan, C. P., Li, S. L., et al. (2019). Grain-Size Classi¯cation by Fabric Support of Coarse Sedimentary Particles: a Case from the Northwest Junggar Basin. *Xinjiang Univ. Nat. Sci. Ed.* 36, 369–378. doi:10.3969/j.issn.1000-1980.2019.03.008

Yin, S. L., Liu, Z. B., Chen, Y. H., and Wu, X. J. (2017). Research progress and sedimentation experiment simulation about alluvial fan: a case study on alluvial fan controlled by debris flow and braided river. *Acta Sedimentol. Sin.* 35, 10–23. doi:10.14027/j.issn.1000-0550.2017.001

Yuan, X. G. (2016). *Characteristics of gravelly sandstone reservoir of Baikouquan formation of Triaassic in Mahu sag[D]*. Hubei: Yangzi university.

Zhang, C. M., Song, X. M., Wang, X. L., Wang, X. L., Zhao, K., Shuang, Q., et al. (2020). Origin and depositional characteristics of supported conglomerates. *Pet. Explor. Dev.* 47, 272–285. doi:10.1234/abcde.67890

Zhang, L. W., Yan, D. T., Liu, W. H., Yang, X. R., Wei, X. S., Xu, H. W, et al. (2019). Sequence strata and coal accumulation of Xishanyao Formation in Tiaohu sag of Santanghu Basin, Sinkiang. *J. China Coal Soc.* 44, 545–556. doi:10.13225/j.cnki.cjxb.2019.02.018

Zhang, Z. L., Tian, J. C., Luo, X. J., and Zhang, J. Q. (2014). Sedimentary Characteristics of Flood Debris Flow and Traction Current in the Lower Shihezi Formation of Permian in the Northern of Ordos Basin. *J. Earth Sci. Environ.* 36, 21–30. doi:10.3969/j.issn.1009-929X.2014.03.003

Zhu, H., Huang, C., Ju, Y., Bu, H., Li, X., Yang, M., et al. (2021). Multi-scale multidimensional characterization of clay-hosted pore networks of shale using FIBSEM, TEM, and X-ray micro-tomography: Implications for methane storage and migration. *Appl. Clay Sci.* 213 (2021), 106239. doi:10.1016/j.clay.2021.106239

Zhu, H. T., Xu, Z. G., Du, X. F., Liu, Q. H., Sun, Z. H., and Zeng, Z. W. (2023). Quantitative reconstruction, classification, and coupling models of paleo-source-sink systems in continental basins. *Pet. Nat. Gas. Geol.* 44, 539–552. doi:10.11781/petnggeology.2023.0

Zhu, X. M., Yang, J. S., and Zhang, X. L. (2004). Application of lithofacies palaeogeography in petroleum exploration. *J. Paleogeogr.* 6, 101–109. doi:10.3969/j.issn.1671-0513.2004.01.014